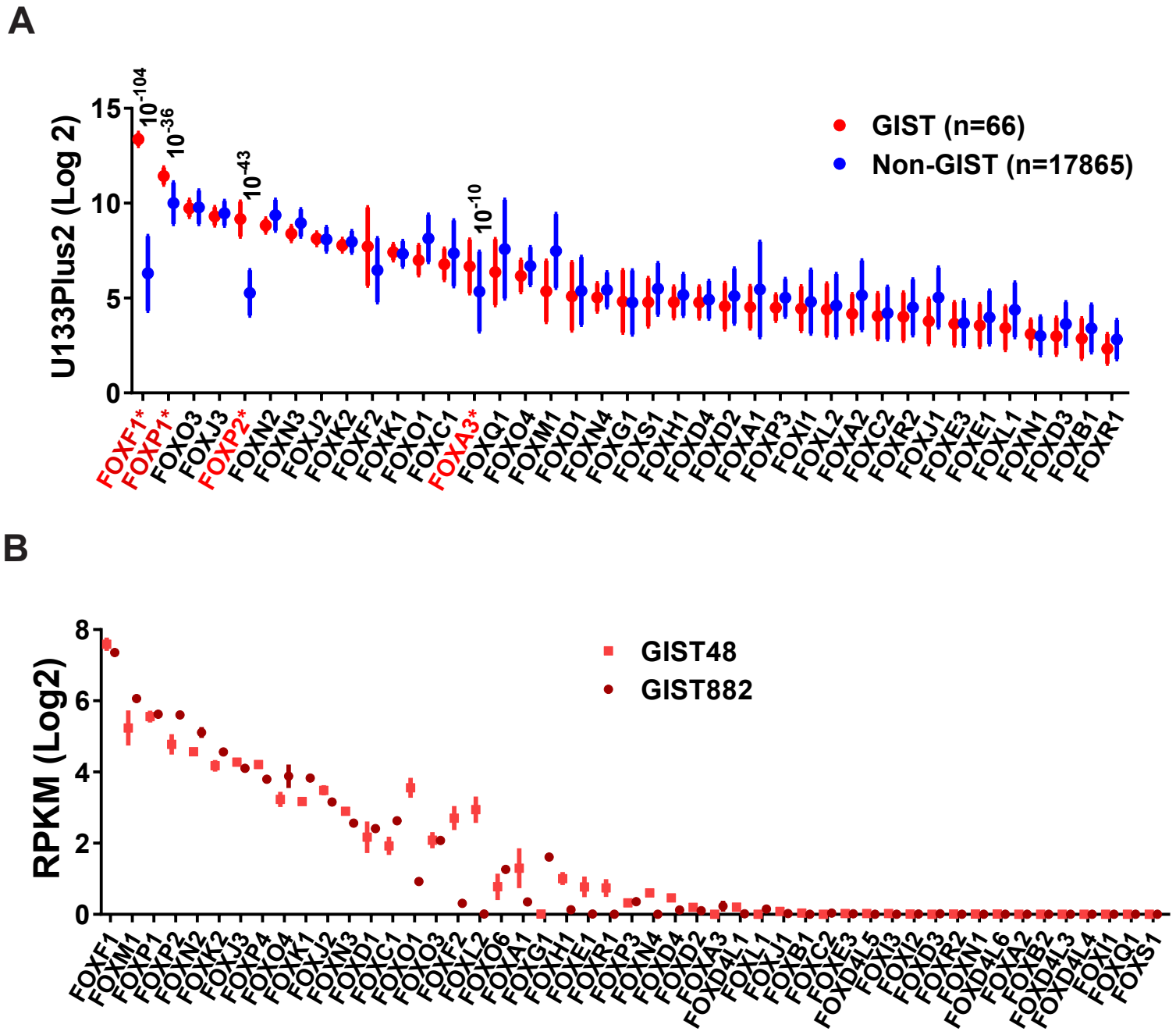

Supplementary Figure S1

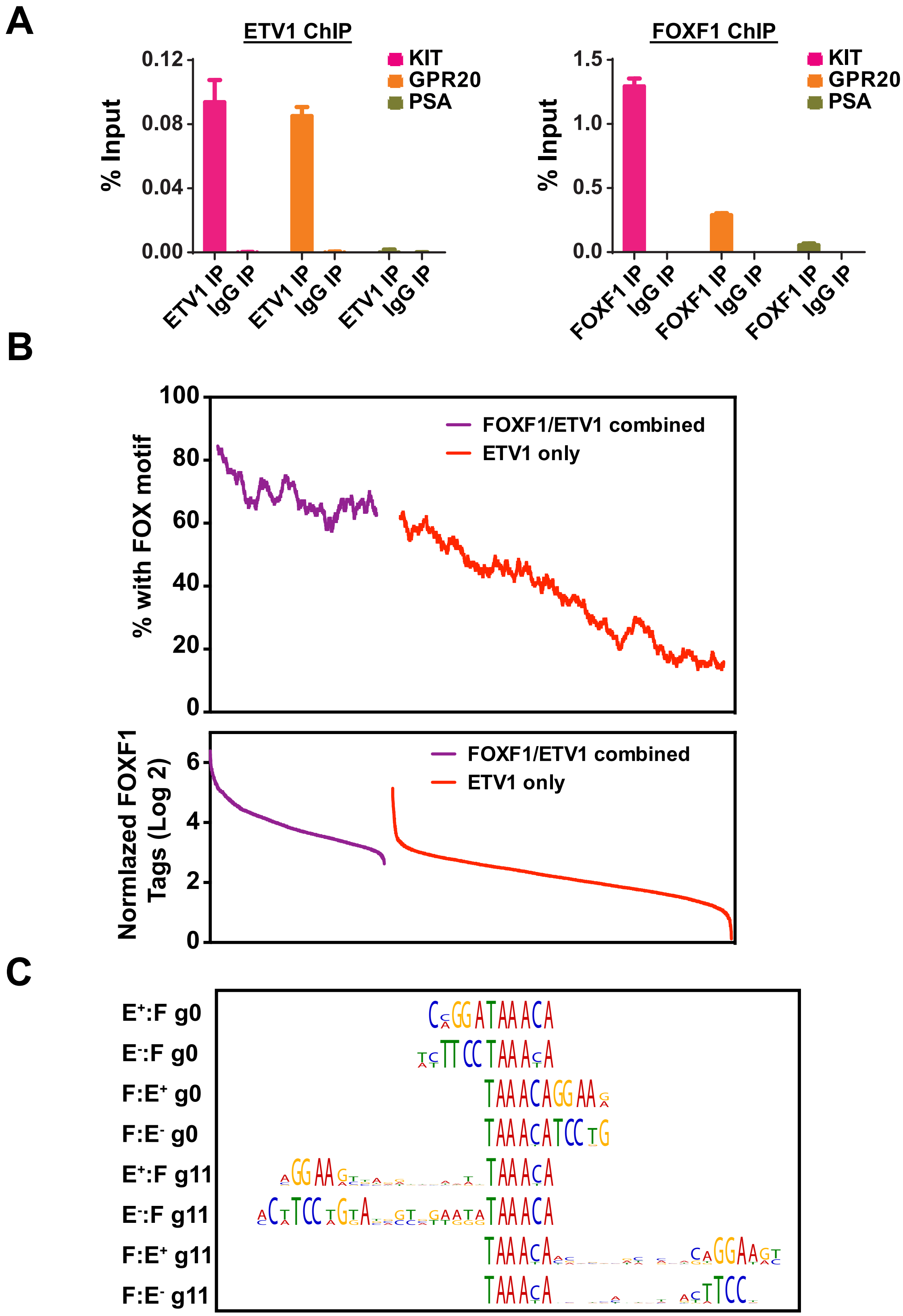

Supplementary Figure S2

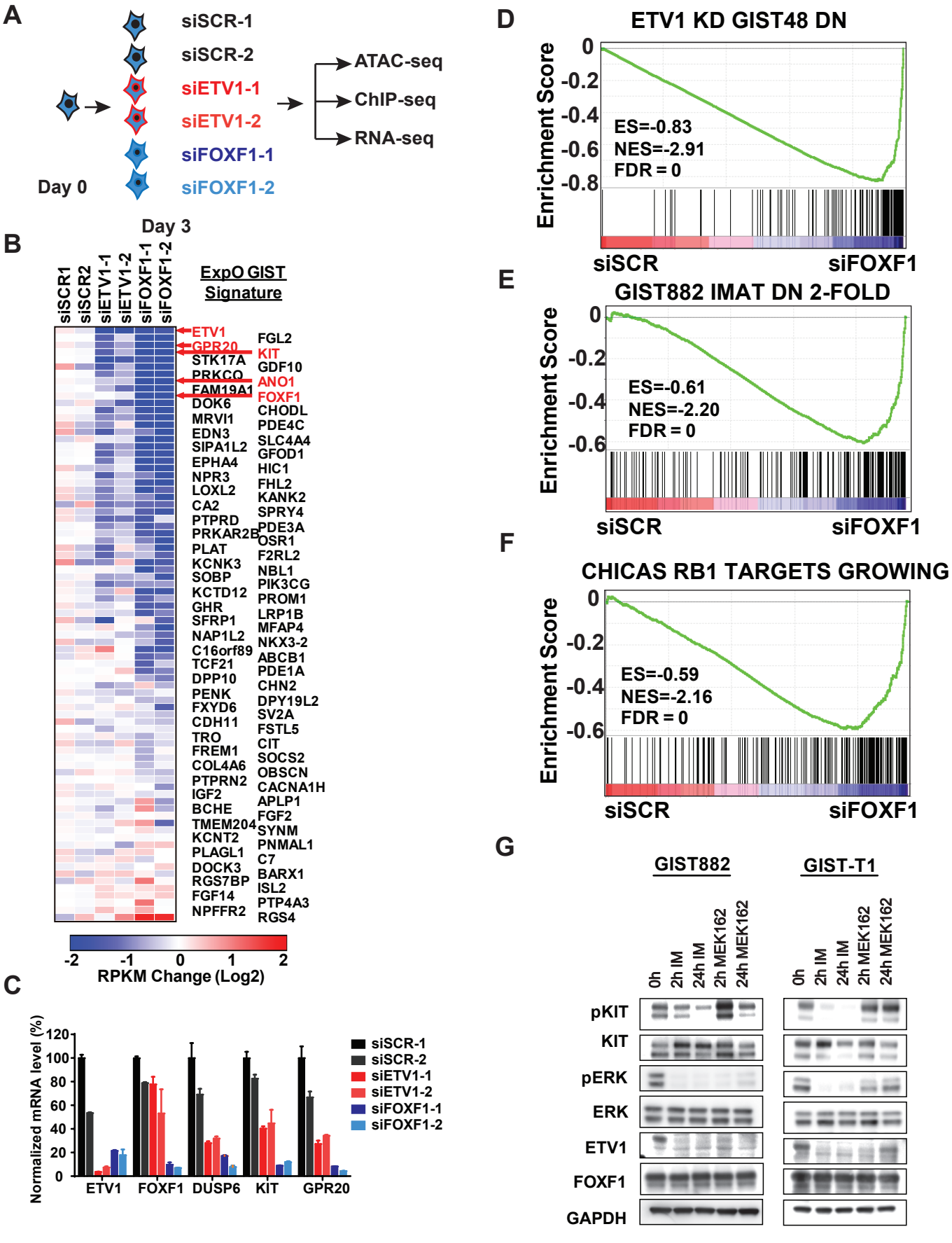

Supplementary Figure S3

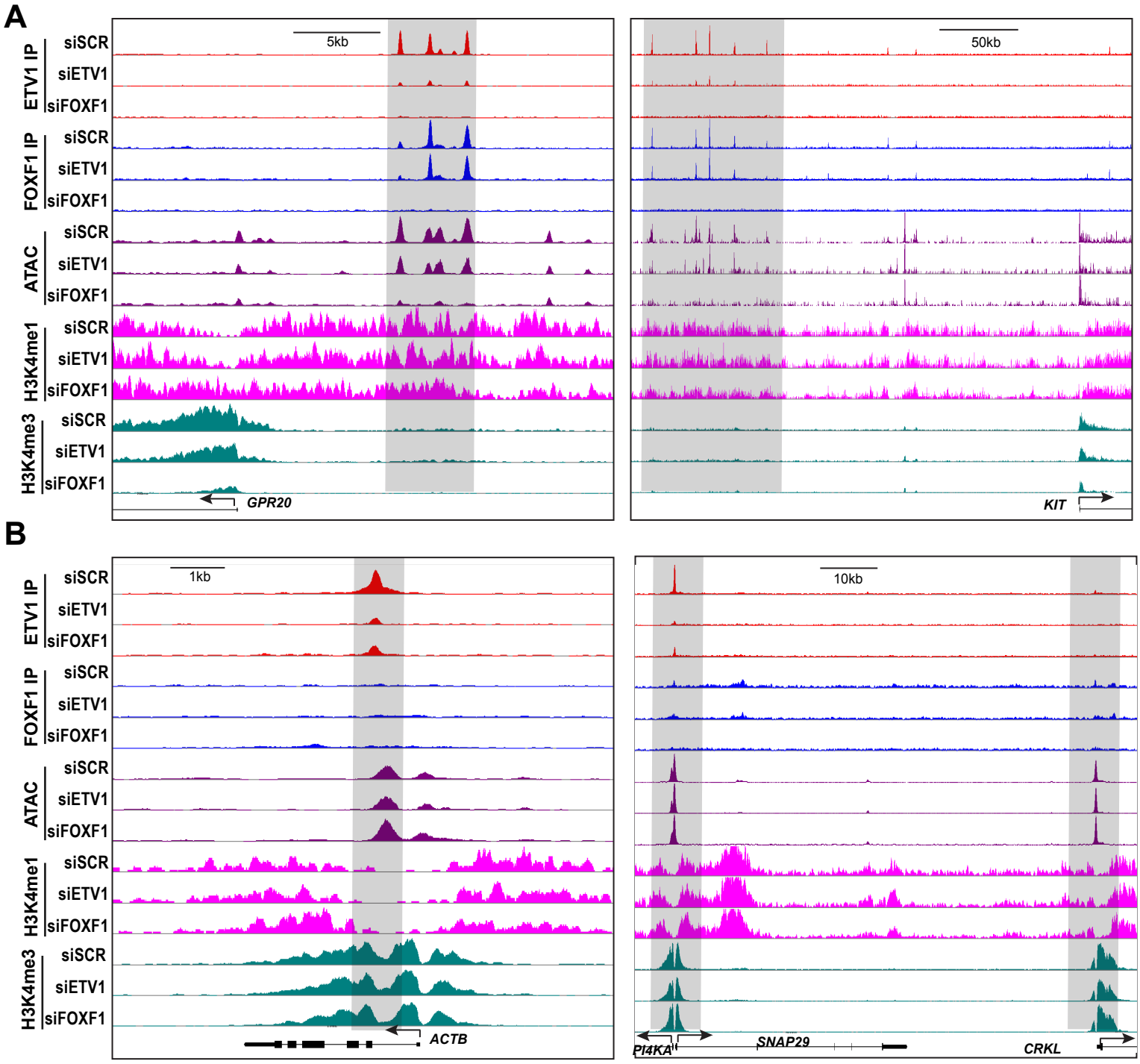

Supplementary Figure S4

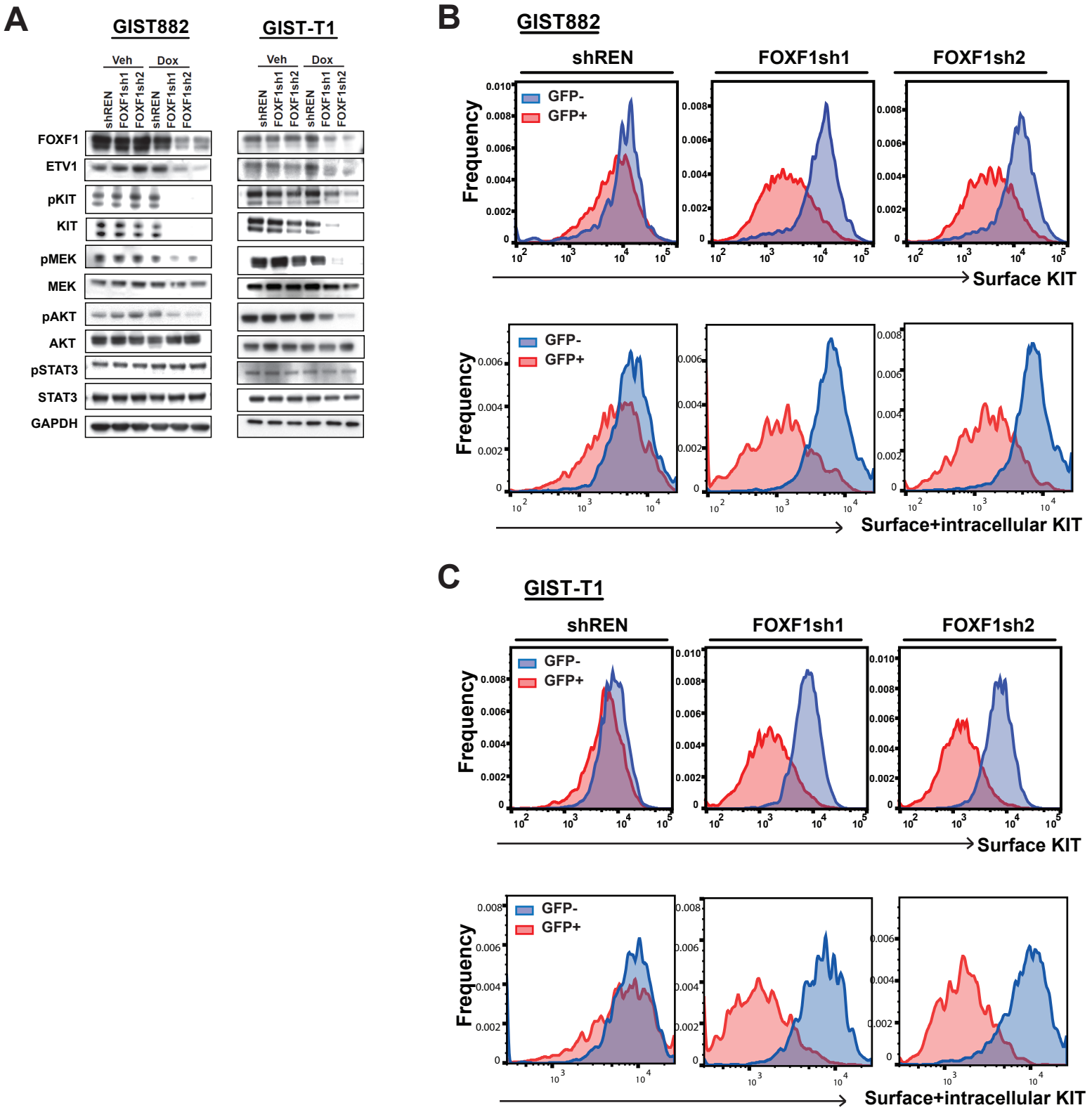

Supplementary Figure S5

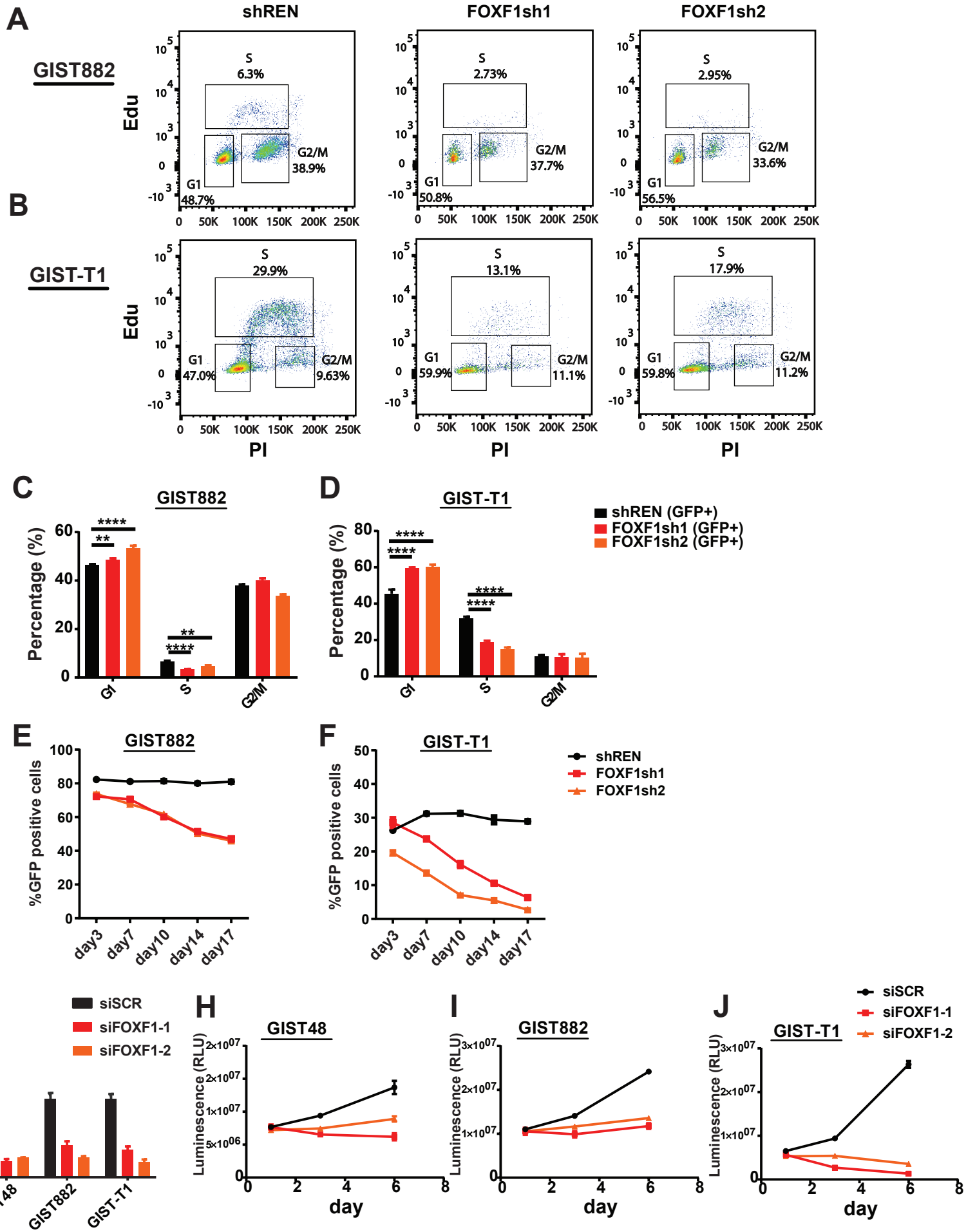

Supplementary Figure S6

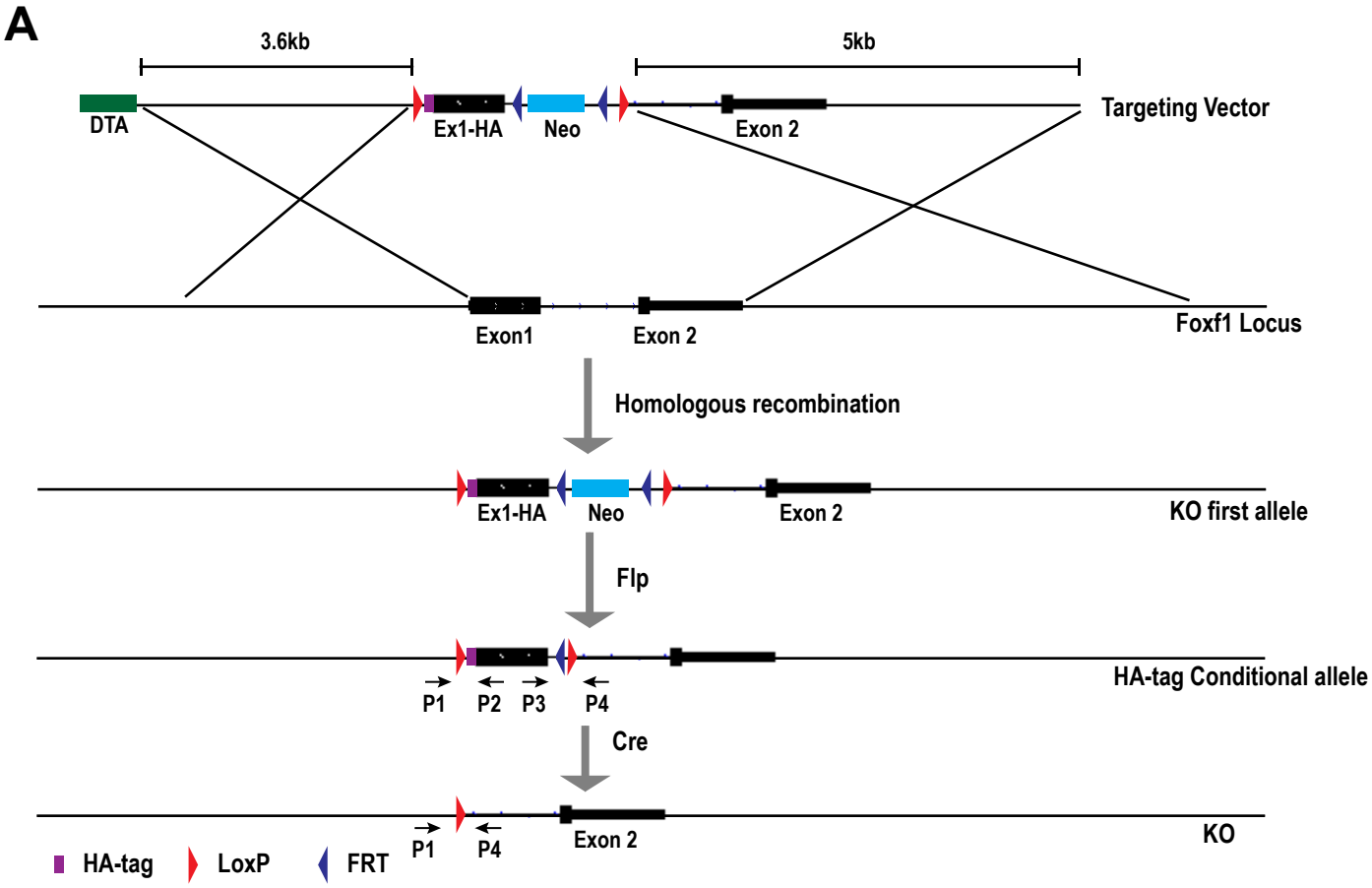

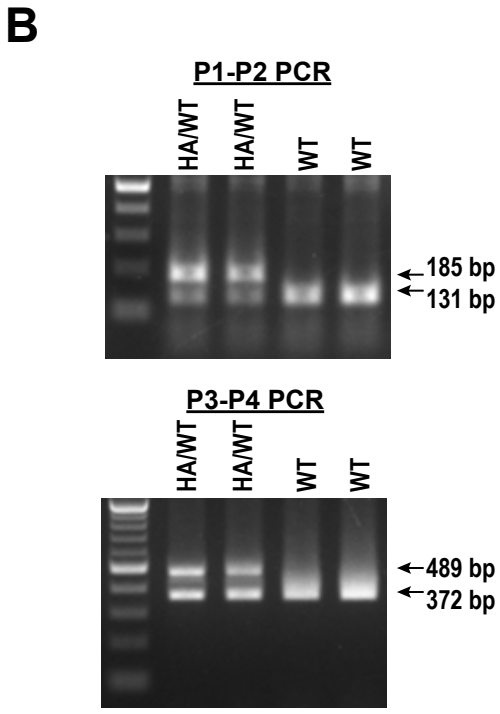

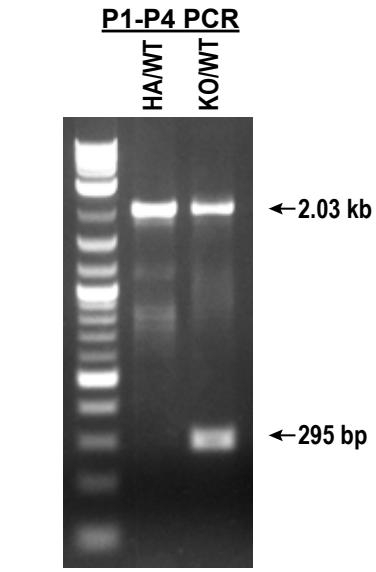

Supplementary Figure S7

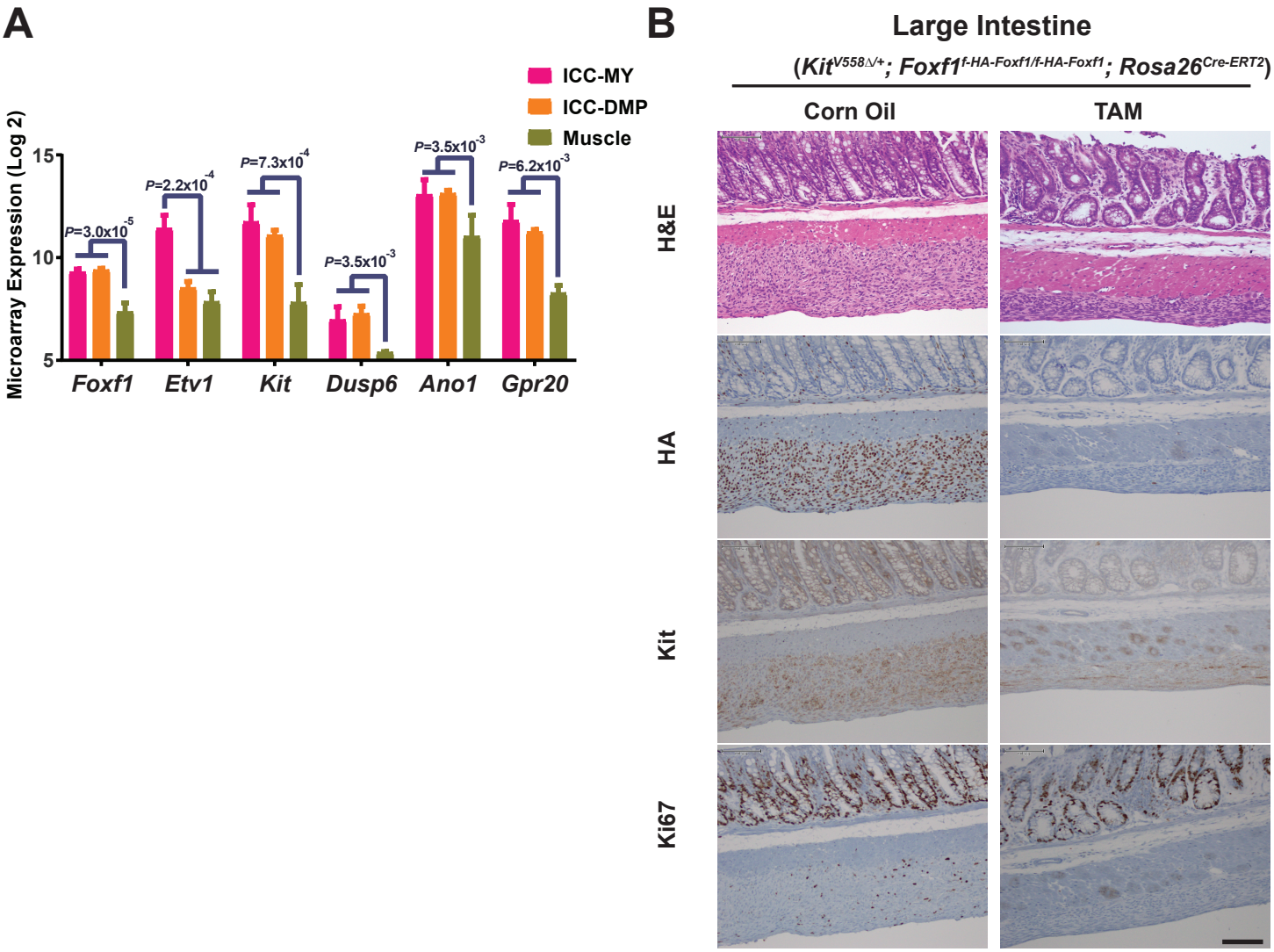

Supplementary Figure S8

Supplementary Figure Legends

Supplementary Figure S1. **Expression of forkhead family transcription factors in GIST. A,** Affymetrix U133Plus2 based gene expression of forkhead transcription factors in 66 GIST (red) and 17,865 non-GIST (blue) tumors from the GENT (Gene Expression database of Normal and Tumor tissues) dataset. Mean ± SD, Student t-test. *P*-value < 10^{-10} shown. **B**, Quantification of gene expression by RNA-seq (Log 2 Reads per Kilobase Mapped, RPKM) of forkhead transcription factors in GIST48 and GIST882 cells. N=2, Mean ± SD.

Supplementary Figure S2. **Motif analysis of the FOXF1 cistrome and validation of FOXF1 binding sites in GIST 48 cells. A**, ChIP-qPCR validation of FOXF1 and ETV1 binding sites by ChIP-seq in GIST48 cells. **B**, FOXF1/ETV1 shared peaks (purple) and ETV1-only peaks (red) sorted by FOXF1 ChIP-seq counts at peak (bottom), showing running average of percent of peaks with FOX motif. **C**, Consensus motif logo of the FOXF1/ETV1 co-localized binding sites by Spaced Motif Analysis (SpaMo), with ETS motif before or after FOX motif, ETS motif in forward (+) or reverse (-) orientation, and gap (g) of 0-bp or 11-bp.

Supplementary Figure S3. FOXF1 regulates *ETV1*, *KIT*, and ETV1- and KIT-dependent transcriptome as well as cell cycle regulated genes. **A**, A schematic of FOXF1- and ETV1-dependent transcriptome and chromatin landscape analyses under siRNA-mediated perturbations of *FOXF1* and *ETV1* in GIST48 cells. **B**, Heatmap of transcriptome changes of genes in the ExpO GIST signature with siRNA-mediated perturbation of *FOXF1* and *ETV1*. **C,** Validation of siRNA-mediated downregulation of *FOXF1*, *ETV1* and their target genes, *DUSP6*, *KIT* and *GPR20*, by qRT-PCR. Error bars: Mean ± SEM. **D-F,** GSEA of transcriptome changes in GIST48 as a result of siRNA-mediated downregulation of *FOXF1* (siFOXF1) compared to scramble controls (siSCR), demonstrating that the ETV1-dependent (ETV1 KD GIST48 DN) (**D**), KIT signaling-dependent (GIST882 IMAT DN 2-FOLD) (**E**) and cell cycle related (CHICAS RB1

TARGETS GROWING) (**F**) transcriptomes are among the most negatively enriched gene set signatures. ES: Enrichment Score; NES: Normalized Enrichment Score; FDR: False Discovery Rate. **G**, Immunoblot of indicated proteins in GIST882 and GIST-T1 cells after treatment with 0.5μM imatinib (IM) or 1μM MEK162 for 2 and 24 hrs.

Supplementary Figure S4. Representative ChIP-seq and ATAC-seq profiles with siRNA-mediated downregulation of *ETV1* and *FOXF1* in GIST48 cells. Normalized ChIP-seq tracks of ETV1 (red), FOXF1 (blue), H3K4me1 (magenta), H3K4me3 (teal) and ATAC-seq tracks (purple) in GIST48 cells transfected with siSCR, siETV1, and siFOXF1. **A**, At lineage specific *GPR20* and *KIT* enhancers co-bound by ETV1 and FOXF1, siFOXF1 caused more decrease in ETV1 binding than siETV1, and loss of ATAC signal. At the associated promoters, H3K4me3 showed decreased width and height of enrichment with both siETV1 and siFOXF1 consistent with decreased transcription of *GPR20* and *KIT*. **B**, At "ETV1-only" *ACTB* enhancer and the bi-directional *PI4KA/SNAP29* promoter, and at the non-ETV1 non-FOXF1 bound *CRKL* promoter, siETV1 caused more decrease in ETV1 binding than siFOXF1. ATAC signal and H3K4me3 signal was unchanged by either siETV1 or siFOXF1 at these loci. **C**, Immunoblots of endogenous ETV1 and FOXF1 immunoprecipitant in GIST cells as indicated.

Supplementary Figure S5. FOXF1 regulates *KIT* expression and signaling. A, Validation of doxycycline inducible shRNA-mediated downregulation of FOXF1 and target proteins, ETV1 and KIT in GIST882 and GIST-T1 cells, as well as components of the MAPK, AKT and STAT3 signaling pathways by immunoblots. **B-C**, Effect of shRNA-mediated *FOXF1* downregulation on cell-surface KIT and total KIT (surface plus intracellular) protein levels by FACS in GIST882 (**B**) and GIST-T1 (**C**) cells.

Supplementary Figure S6. FOXF1 regulates cell cycle progression and is required for growth and proliferation of GIST cells *in vitro*. A-B, Effect of shRNA-mediated *FOXF1*

downregulation on cell cycle progression using DNA content and EdU labeling in GIST882 and GIST-T1 cells. **C-D**, Quantification of percentages of cells in G1, S, and G2/M cycle phase. N=3, Mean ± SD, Student t-test. ***P*<0.01, *****P*<0.0001. **E-F**, Effect of shRNA-mediated *FOXF1* downregulation on cell growth in competition assays of GIST882 (**E**) and GIST-T1(**F**). Day 0 is day of doxycycline addition. **G,** qRT-PCR validation of *FOXF1* downregulation by two independent siRNA in GIST 48, GIST 882 and GIST T1 cells that were subsequently analyzed for growth in **H-J**. N=3, Mean ± SD. **H-J**, Effect of siRNA-mediated *FOXF1* downregulation on cell proliferation of GIST48(**H**), GIST882 (**I**) and GIST-T1 (**J**) in independent growth assays. N=3, Mean ± SD.

Supplementary Figure S7. Generation of the *Foxf1*$^{f\text{-}HA\text{-}Foxf1}$ allele. A, Schematic of gene-targeting. An HA-tag was introduced to the amino-terminus of Foxf1 in exon 1. The exon was placed between two LoxP sites (red triangle), adjacent to a neomycin cassette flanked by FRT sites (blue triangle). The 3' homology arm is flanked by the diphtheria toxin cassette (DTA) for negative selection of non-homologous integration. Heterozygous KO-first mice was crossed with Actb-FlpE mice to excise the neomycin cassette and generate the conditional tagged *Foxf1*$^{f\text{-}HA\text{-}Foxf1}$ allele. **B**, PCR using P1-P2 flanking 5' LoxP site and P3-P4 flanking the 3' LoxP site in two heterozygous and two wild-type mice. **C**, PCR using P1-P4 that flank the entire exon 1 in heterozygous cells before and after Cre-mediated deletion.

Supplementary Figure S8. *Foxf1* expression in mouse GI tract and *Foxf1* ablation reduces mutant *Kit*-mediated hyperplasia of mouse large intestine. A, Gene expression of *Foxf1*, *Etv1*, and ICC-GIST lineage specific genes, *Kit*, *Dusp6*, *Ano1*, *Gpr20* in different ICC subclasses (ICC-MY: myenteric ICCs; ICC-SMP: submucosal ICCs) and the smooth muscle from mouse small intestine from GSE7809. **B,** Representative images of H&E, IHC of indicated markers of mouse large intestine derived from *Kit*$^{V558\Delta/+}$*; Foxf1*$^{f\text{-}HA\text{-}Foxf1/f\text{-}HA\text{-}Foxf1}$*; Rosa26*$^{Cre\text{-}ERT2}$

treated with either corn oil control or TAM. Scale bar: 100 μm. All *P* values are as indicated and significant by two-tailed and unpaired *t* test.